RSC Advances

ROYAL SOCIETY OF CHEMISTRY

www.rsc.org/advances

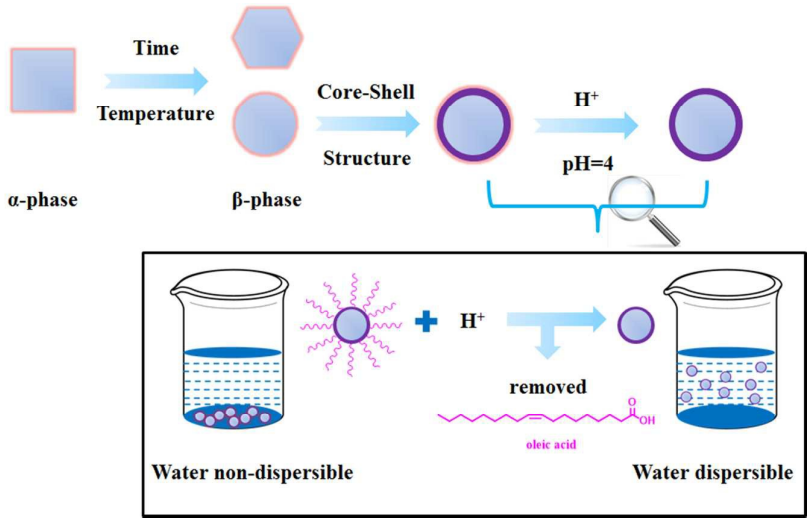

Ytterbium and erbium co-doped sodium yttrium fluoride ($NaYF_4$: Er^{3+}, Yb^{3+}) rare-earth upconversion nanoparticles (UCNPs) with α and β phases were prepared. UCNPs with core-shell structure were prepared and modified to be hydrophilic by ligand-free hydrophilic modification.

Journal Name

ARTICLE

Synthesis and characterization of upconversion nanoparticles with shell structure and ligand-free hydrophilic modification

Received 00th January 20xx,
Accepted 00th January 20xx

DOI: 10.1039/x0xx00000x

www.rsc.org/

Di Kang†[a], Xiaoyan Song†[b] and Jinfeng Xing[a]*

Ytterbium and erbium co-doped sodium yttrium fluoride ($NaYF_4$: Er^{3+}, Yb^{3+}) rare-earth upconversion nanoparticles (UCNPs) with different phases were prepared and characterized. The luminescence intensity of UCNPs can be enhanced by coating a uniform layer of the shell. The crystal structure, morphology and upconversion spectra of the sample were investigated using X-ray powder diffractometer, transmission electron microscope, and laser upconversion spectrometer with 980 nm diode laser. Finally, UCNPs with core-shell structure were modified to be hydrophilic by ligand-free hydrophilic modification. Moreover, the water dispersible UCNPs have much stronger luminescence compared with hydrophobic UCNPs.

1 Introduction

Rare-earth upconversion nanoparticles (UCNPs) excited by near-infrared light exhibit a unique narrow photoluminescence with higher energy,[1, 2] in which the low-energy photons transfer into a higher-energy photons through a multi-step.[3] Compared with the conventional down-conversion material such as organic dyes and quantum dots (QDs), UCNPs have several advantages such as high light penetration depth in tissues, no photo-damage to living organisms, weak autofluorescence from cells or tissues, low background light, high sensitivity for detection, minimal photobleaching and low phototoxicity.[4-6] Therefore, UCNPs can be applied in various biomedical applications, including immunoassays, biomedical imaging, molecular sensing, X-ray computed tomography (CT), and photodynamic therapy (PDT).[3, 7-10]

UCNPs with high-quality are important to meet biomedical applications. UCNPs are composed of three components including a host matrix, a sensitizer and an activator. An ideal host matrix should have low lattice photon energies as a prerequisite to minimize non-radiative losses and maximize the radiative emission.[11] Among the available types of upconversion host materials, fluoride such as $NaYF_4$ was proved to be the best choice due to their relatively low phonon energy and excellent chemical stability.[12-14] Most of the attention has been focused on the synthesis of high-quality nanoparticles such as cubic (α-) and hexagonal (β-) $NaYF_4$.[15-18] In all of the upconversion materials, cubic (α-) and hexagonal (β-) $NaYF_4$ have been reported as the most efficient UCL host materials, especially for Yb^{3+}/Er^{3+} upconversion systems.[18-20] However, the properties of the upconversion nanoparticles are not only determined by their phase, but also by their structure, size, morphology, synthesis process and composition.[17, 21] Therefore, it needs to have a deeper analysis and comparison of cubic (α-) and hexagonal (β-) $NaYF_4$. It was confirmed that luminescence of upconversion nanoparticles can be enhanced only by adjusting phases but also by coating shell.[22, 23]

Usually, synthetic approaches for UCNPs involved the use of organic capping ligands. Therefore, UCNPs are hydrophobic.[21, 24-27] Due to the hydrophobicity of UCNPs, they are hard to be applied in biomedical field. Several strategies to develop water dispersible UCNPs have been reported such as encapsulation by SiO_2,[28-30] ligand exchange,[31] ligand oxidation reaction,[32] and surface modification.[33, 34] However, the precise control over the thickness and shape of the encapsulating SiO_2 layer are difficult to be precisely controlled, resulting in a relatively larger hydrodynamic particle radius.[35] The methods of Ligand exchange and ligand oxidation are limited to a specific class of UCNPs capped with ligand molecules containing unsaturated carbon-carbon bonds in their long alkyl chains.[11] Ligand-free has recently been used to prepare water dispersible UCNPs, the UCNPs obtained are uniform, which is a convenient, safe and low-cost method to remove the oleate ligand and to

Address here.
Address here.
Address here.
† Footnotes relating to the title and/or authors should appear here.
Electronic Supplementary Information (ESI) available: [details of any supplementary information available should be included here]. See DOI: 10.1039/x0xx00000x

obtain highly water dispersible UCNPs with strong luminescence.[36]

In this study, two phases of ytterbium and erbium co-doped sodium yttrium fluoride nanoparticles ($NaYF_4$: Er^{3+}, Yb^{3+}) were prepared to examine their luminescence properties, size and morphology under different synthetic conditions. To further enhance the luminescence intensity, UCNPs with core-shell structure were also prepared. Finally, UCNPs with core-shell structure were modified to be hydrophilic by ligand-free hydrophilic modification. Importantly, the water dispersible UCNPs have much stronger luminescence compared with hydrophobic UCNPs.

2 Experimental

2.1 Materials

All chemicals were of analytical grade and used as received without further purification. Deionized water was used throughout. $Y(CH_3CO_2)_3$ (99.9% trace metals basis), $Yb(CH_3CO_2)_3$ (99.9% trace metals basis) and $Er(CH_3CO_2)_3$ (99.9% trace metals basis) were supplied by Sigma-Aldrich. Oleic acid (technical grade, 90%), 1-Octadecene (technical grade, 90%) and NaOH (reagent grade, ≥98%) were supplied by Aladdin company. Methanol (reagent grade, ≥99.5%), Ethanol (reagent grade, ≥99.7%), Cyclohexane (reagent grade, ≥99.5%), HCl (reagent grade, 36%~38%), Acetone (reagent grade, ≥99.5%), Ethyl ether (reagent grade, ≥99.5%) and NH_4F (ACS reagent, ≥98%) were purchased from Jiangtian Chemical Technology Co.,Ltd (Tianjin China).

2.2 Synthesis of α-$NaYF_4$: Er^{3+}, Yb^{3+} and β-$NaYF_4$: Er^{3+}, Yb^{3+} Nanocrystals

Firstly, a water solution (3 mL) containing $Y(CH_3CO_2)_3$ (0.4 mmol), $Yb(CH_3CO_2)_3$ (0.392 mmol) and $Er(CH_3CO_2)_3$ (0.008 mmol) was added to a 50 mL flask containing oleic acid (8 mL) and 1-octadecene (12 mL). Then the mixture was heated at 150 ^oC while stirring for 1 h to form lanthanide oleate complexes and remove water and then cooled down to room temperature. Subsequently, a methanol solution (8.8 mL) containing NH_4F (2.64 mmol) and NaOH (2 mmol) was added and stirred at 50 ^oC for 1 h. After the reaction temperature was increased to 100 ^oC, the methanol and water were removed from the reaction mixture. Then the solution was heated to 300 ^oC and maintained at this temperature under an argon atmosphere for 1.0-1.7 h, and then the mixture was cooled down to room temperature. The resulting nanoparticles were precipitated out through an addition of ethanol, collected by centrifugation, washed with ethanol, and finally redispersed in 8 mL of cyclohexane.

2.3 Synthesis of β-$NaYF_4$: Er^{3+}, Yb^{3+} Nanospheres

Firstly, a water solution (3 mL) containing $Y(CH_3CO_2)_3$ (0.8 mmol), $Yb(CH_3CO_2)_3$ (0.18 mmol) and $Er(CH_3CO_2)_3$ (0.02 mmol) was added to a 50 mL flask containing oleic acid (6 mL) and 1-octadecene (15 mL). Then the mixture was heated at 150 ^oC while stirring for 1 h to form lanthanide oleate complexes and remove water and then cooled down to room temperature. Subsequently, a methanol solution (8.8 mL) containing NH_4F (2.64 mmol) and NaOH (2 mmol) was added and stirred at 50 ^oC for 1 h. After the reaction temperature was increased to 100 ^oC, the methanol and water were removed from the reaction mixture. Then the solution was heated to 300 ^oC or 320 ^oC and maintained at this temperature under an argon atmosphere for 1.5 h or 2.0 h, and then the mixture was cooled down to room temperature. The resulting nanoparticles were precipitated out through an addition of ethanol, collected by centrifugation, washed with ethanol, and finally redispersed in 8 mL of cyclohexane.

2.4 Synthesis of $NaYF_4$:Er^{3+}, Yb^{3+}@ $NaYF_4$ Nanospheres

A water solution (2 mL) containing $Y(CH_3CO_2)_3$ (0.4 mmol) was added to a 50 mL flask containing oleic acid (6 mL) and 1-octadecene (15 mL). The mixture was then heated at 150 ^oC for stirring for 1 h and then cooled down to 50 ^oC. The β-$NaYF_4$: Er^{3+}, Yb^{3+} nanospheres in cyclohexane were added along with a 6 mL methanol solution of NH_4F (1.76 mmol) and NaOH (1.1 mmol). The resulting mixture was stirred at 50 ^oC for 1 h, and then the reaction temperature was increased to 100 ^oC to remove the methanol and cyclohexane. After that the solution was heated at 300 ^oC under an argon flow for 1.5 h and then cooled to room temperature. The resulting nanoparticles were precipitated out by the addition of ethanol, collected by centrifugation, washed with ethanol, and redispersed in cyclohexane.

2.5 Synthesis of water dispersible $NaYF_4$:Er^{3+}, Yb^{3+}@$NaYF_4$ Nanospheres

Water dispersible β-$NaYF_4$:Er^{3+}, Yb^{3+}@$NaYF_4$ nanospheres were obtained by the previously reported strategy.[36] β-$NaYF_4$: Er^{3+}, Yb^{3+}@$NaYF_4$ nanospheres were dispersed in a 10 mL aqueous solution. The reaction was performed with stirring for 2 h while maintaining the pH at 4 by adding a solution of 0.1 M HCl. After the reaction was completed, the mixture solution was extracted with diethyl ether for three times. The resulting nanoparticles were precipitated out by the addition of acetone, collected by centrifugation and redispersed in deionized water.

2.6 Characterization

The phase purity of the products was examined by Powder X-ray diffraction (XRD) on D8-Focus using Cu Kα radiation (λ=1.5406 Å). The size and morphology of the nanocrystals were determined by JEM-2100F transmission electron microscope (TEM) at 200 kV. Samples were prepared by placing a drop of a dilute cyclohexane dispersion of nanocrystals on the surface of a copper grid. UC emission spectra were obtained using 980 nm diode laser with a 0.75 W/cm^2 of laser power density (UCNPs concentration is 1 wt % in cyclohexane or water). The ^1H NMR spectrum of oleic acid and the oleate-capped $NaYF_4$: Er^{3+}, Yb^{3+}@$NaYF_4$ Nanospheres dispersed in $CDCl_3$ and the oleate-free $NaYF_4$: Er^{3+}, Yb^{3+}@$NaYF_4$ Nanospheres dispersed in D_2O were recorded on 500 MHz (Varian INOVA) NMR spectrometer as solvent containing a small amount of TMS as internal standard. FTIR spectra were performed on a WQF-510A instrument using the pressed KBr pellet.

3 Results and Discussion

3.1 Characterization of α-$NaYF_4$: Er^{3+}, Yb^{3+} and β- $NaYF_4$: Er^{3+}, Yb^{3+} Nanocrystals

Fig. 1 shows the powder XRD patterns of cubic (α-) and hexagonal (β-) $NaYF_4$: Er^{3+}, Yb^{3+} UCNPs prepared at different reaction time. When the reaction time was 1 h, all the diffraction peaks could be indexed to those of a pure phase-cubic $NaYF_4$ crystal structure (JCPDS standard card No. 27-1426), indicating that cubic (α-) $NaYF_4$: Er^{3+}, Yb^{3+} UCNPs were prepared. When the reaction time reached 1.5 h, transformation of $NaYF_4$ nanocrystals from α- to β-phase appeared. The X-ray diffraction pattern of $NaYF_4$: Er^{3+}, Yb^{3+} samples could be indexed as a mixture of the cubic (JCPDS standard card No. 27-1426) and hexagonal (JCPDS standard card No. 28-1192) phases of $NaYF_4$, demonstrating that the transformation from cubic to hexagonal indeed occurred. The pure hexagonal phase of $NaYF_4$ was obtained as the reaction time prolonged to 1.7 h (JCPDS standard card No. 28-1192).

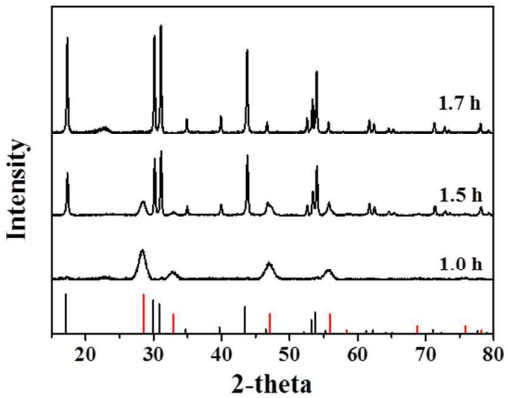

Fig. 1 XRD patterns of $NaYF_4$: Er^{3+}, Yb^{3+} nanocrystals prepared at different reaction time as well as the standard JCPDS No 27-1426 of α-$NaYF_4$: Er^{3+}, Yb^{3+} (red line) and JCPDS No 28-1192 of β- $NaYF_4$: Er^{3+}, Yb^{3+} (black line) (Note that Cu K*α* radiation was used for the XRD measurement).

Fig. 2A-C exhibits the TEM images of cubic (α-) and hexagonal (β-) $NaYF_4$: Er^{3+}, Yb^{3+} UCNPs prepared at 300 °C with various reaction times from 1 h to 1.7 h. It can be observed that all of the nanoparticles have a uniform particle size around 43 nm and good monodisperse. The morphology of UCNPs translates from cube to hexagon with reaction time increasing. When the reaction time reaches 1.5 h, the translation of UCNPs from cube to hexagon obviously occurs. In the UCNPs with cubic structure, the cation sites are equal and the Na and Y atoms randomly distribute in the cationic sublattice, while in the UCNPs with hexagonal structure, there are three different cation sites. Therefore, cubic α-phase is a metastable high-temperature phase and hexagonal β-phase is a thermodynamically stable low-temperature phase.[21, 37, 38] The transformation process from the cubic phase to hexagonal phase is one evolving from disorder to order process, indicating that the transformation from cubic to hexagonal phase is the thermodynamic process and the transformation of disorder to order is a process of growth kinetics.[21]

Under 980 nm laser excitation, Er^{3+} ions in $NaYF_4$ nanocrystals exhibit dual emission bands (green and red).[39] Upconversion spectra of $NaYF_4$: Er^{3+}, Yb^{3+} UCNPs prepared at different reaction time for 300 °C are shown in Fig. 2D. Three emissions bands around 520, 540 and 650 nm are ascribed to $^2H_{11/2}\rightarrow{}^4I_{15/2}$, $^4S_{3/2}\rightarrow{}^4I_{15/2}$ and $^4F_{9/2}\rightarrow{}^4I_{15/2}$ transitions of Er^{3+} ion, respectively.[13, 40] It can be clearly observed that the relative intensity of emissions (520 nm, 540 nm and 650 nm) varies with the reaction time. The luminescence intensity of UCNPs increases with the reaction time. It is suggested that the luminescence intensity can be enhanced by prolonging the reaction time due to the increase of β-$NaYF_4$. It was confirmed that the crystal structure of the β-phase favours the emission of the dopant ions more than that of the α-phase. Naturally, β-$NaYF_4$ has a stronger luminescence intensity.[41]

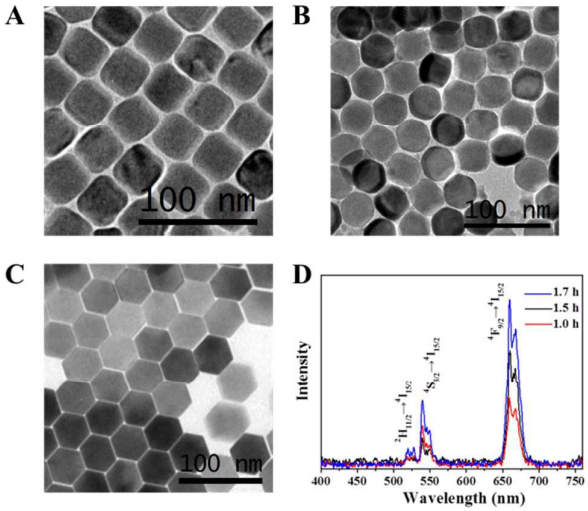

Fig. 2 TEM images of $NaYF_4$: Er^{3+}, Yb^{3+} UCNPs prepared at different reaction time for 300 °C. (A) 1.0 h; (B) 1.5 h; (C) 1.7 h; (D) Upconversion spectra of $NaYF_4$: Er^{3+}, Yb^{3+} UCNPs prepared at different reaction time for 300 °C. All of nanoparticles were excited at 980 nm with a diode laser.

3.2 Characterization of β-$NaYF_4$: Er^{3+}, Yb^{3+} Nanospheres

The x-ray diffraction (XRD) pattern results of the β-$NaYF_4$: Er^{3+}, Yb^{3+} nanospheres are shown in Fig. 3. All the diffraction peaks could be indexed to a pure phase-hexagonal $NaYF_4$ nanospheres structure (JCPDS standard card No. 28-1192). No diffraction peaks corresponding to cubic phases or other impurities appear, indicating the successful synthesis of pure hexagonal-phase $NaYF_4$ nanospheres. Moreover, it can be deduced that the β-$NaYF_4$: Er^{3+}, Yb^{3+} nanospheres own highly crystalline in nature from the intensity of the peaks. Furthermore, as shown in Fig.3, comparing with samples at different reaction temperature, it can be found that the crystalline of β-$NaYF_4$: Er^{3+}, Yb^{3+} nanospheres could be improved by increasing reaction temperature or prolonging reaction time. However, there is no influence on the phase of β-$NaYF_4$: Er^{3+}, Yb^{3+} nanospheres.[42]

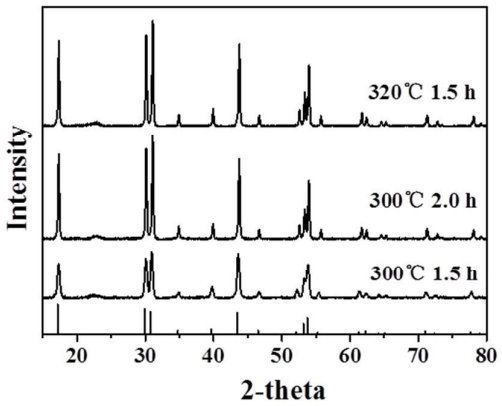

Fig. 3 XRD patterns of $NaYF_4$: Er^{3+}, Yb^{3+} nanospheres prepared at different reaction time and temperature as well as the standard JCPDS No 28-1192 of β-$NaYF_4$: Er^{3+}, Yb^{3+} (Note that Cu Kα radiation was used for the XRD measurement).

Fig. 4A-C exhibits the TEM images of hexagonal (β-) $NaYF_4$: Er^{3+}, Yb^{3+} nanospheres prepared at various conditions. It can be clearly observed that uniform hexagonal nanospheres at 25 nm were obtained. Under NIR 980 nm laser excitation, the spectra of $NaYF_4$: Er^{3+}, Yb^{3+} UCNPs prepared at different conditions are shown in Fig. 4D. All $NaYF_4$: Er^{3+}, Yb^{3+} UCNPs exhibit three emissions bands around 520, 540 and 650 nm. It can be seen that the luminescence intensity of $NaYF_4$: Er^{3+}, Yb^{3+} UCNPs could be improved by increasing reaction temperature or prolonging reaction time.

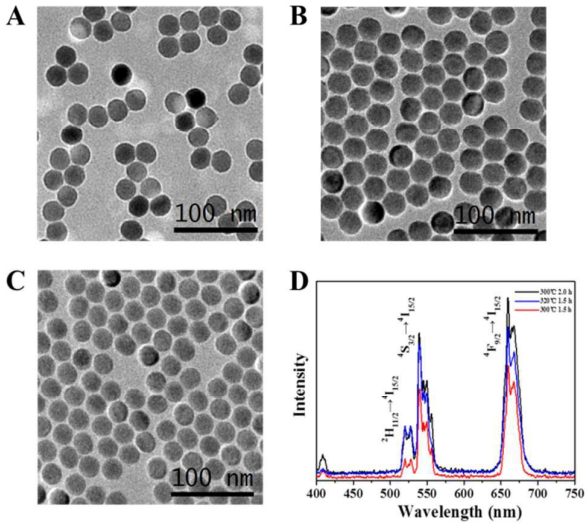

Fig. 4 TEM images of $NaYF_4$: Er^{3+}, Yb^{3+} nanospheres prepared at different reaction conditions. (A) 300 °C, 1.5 h; (B) 320 °C, 1.5 h; (C) 300 °C, 2.0 h; (D) Upconversion spectra of $NaYF_4$: Er^{3+}, Yb^{3+} nanospheres prepared at different reaction temperature for 1.5 h. All of nanoparticles were excited at 980 nm with a diode laser.

3.3 Characterization of $NaYF_4$: Er^{3+}, Yb^{3+}@$NaYF_4$ Nanospheres

Lanthanide-doped UCNPs often suffer from much strong deleterious surface quenching effects due to their high surface-to-volume ratio. The surface quenching can be solved by forming a uniform shell over the core. Fig. 5A-B exhibits the TEM images of hexagonal $NaYF_4$: Er^{3+}, Yb^{3+} nanospheres and hexagonal $NaYF_4$: Er^{3+}, Yb^{3+} @$NaYF_4$ nanospheres. It can be clearly observed that the core is coated by a uniform layer of the shell. The x-ray diffraction (XRD) pattern result of the β-$NaYF_4$: Er^{3+}, Yb^{3+}@$NaYF_4$ nanospheres is shown in Fig. 5C. All the diffraction peaks could be indexed to a pure phase-hexagonal $NaYF_4$ nanospheres structure (JCPDS standard card No. 28-1192). Fig. 5D shows the emission spectra of $NaYF_4$: Er^{3+}, Yb^{3+} and $NaYF_4$: Er^{3+}, Yb^{3+}@$NaYF_4$. It clearly reveals that the relative intensity of emissions varies with different structures. When the $NaYF_4$: Er^{3+}, Yb^{3+} was coated by a layer of the shell, its luminescent intensity increases an order of magnitude. The reason is that the characteristic optical features (such as relative emission intensities) of these nanoparticles can be retained by the effective protection of dopant ions through the inert layer coating.[23]

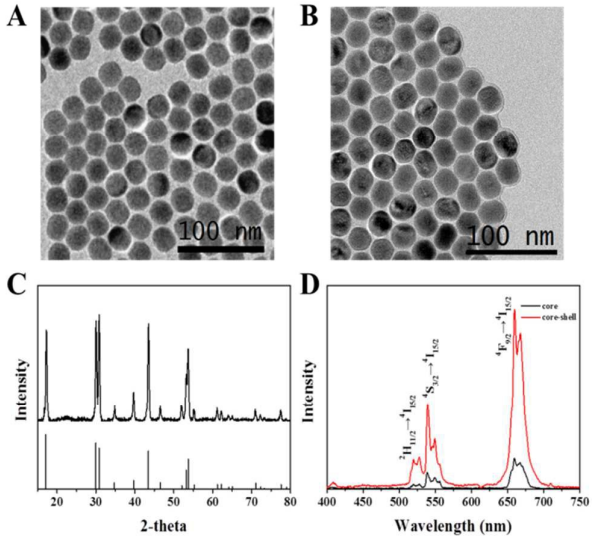

Fig. 5 TEM images of (A) $NaYF_4$: Er^{3+}, Yb^{3+} nanospheres and (B) $NaYF_4$: Er^{3+}, Yb^{3+}@$NaYF_4$ nanospheres; (C) XRD patterns of $NaYF_4$: Er^{3+}, Yb^{3+}@$NaYF_4$ nanospheres and the standard JCPDS No 28-1192 of β-$NaYF_4$: Er^{3+}, Yb^{3+} (Note that Cu Kα radiation was used for the XRD measurement); (D) Upconversion spectra of $NaYF_4$: Er^{3+}, Yb^{3+} nanospheres and $NaYF_4$: Er^{3+}, Yb^{3+}@$NaYF_4$ nanospheres. All of nanoparticles were excited at 980 nm with a diode laser.

3.4 Characterization of water dispersible $NaYF_4$: Er^{3+}, Yb^{3+}@$NaYF_4$ Nanospheres

To achieve water dispersible $NaYF_4$: Er^{3+}, Yb^{3+}@$NaYF_4$ nanoparticles, the oleate-capped $NaYF_4$: Er^{3+}, Yb^{3+}@$NaYF_4$ nanoparticles were modified with a simple Ligand-free method.[36] The UCNPs could exist stably in water for one week. ^{1}HNMR spectra of oleate, oleate-capped $NaYF_4$: Er^{3+}, Yb^{3+}@$NaYF_4$ nanoparticles and water dispersible $NaYF_4$: Er^{3+}, Yb^{3+}@$NaYF_4$ nanoparticles are shown in Fig. 6A. It can be found that the oleate ligand was completely removed from oleate-capped $NaYF_4$: Er^{3+}, Yb^{3+}@$NaYF_4$ nanoparticles though ligand-free method. FTIR spectra of oleate, oleate-capped $NaYF_4$: Er^{3+}, Yb^{3+}@$NaYF_4$ nanoparticles and water dispersible $NaYF_4$: Er^{3+}, Yb^{3+}@$NaYF_4$ nanoparticles are shown in Fig. 6B. The transmission bands at 2929 and 2855 cm^{-1} are attributed to the asymmetric and symmetric stretching vibrations of methylene groups (CH_2) in the long alkyl chain of OA. Two bands at 1458 and 1568 cm^{-1} in OA-UCNPs are attributed to the asymmetric and the symmetric stretches of -COO-. The

characteristic bands corresponding to OA almost disappear, demonstrating that OA was removed from the surface of UCNPs. Fig. 6c shows the upconversion emission spectra of $NaYF_4$: Er^{3+}, Yb^{3+}@$NaYF_4$ nanospheres in water. $NaYF_4$: Er^{3+}, Yb^{3+} UCNPs exhibit emissions bands around 520, 540 and 650 nm, which were ascribed to $^2H_{11/2}\rightarrow{}^4I_{15/2}$, $^4S_{3/2}\rightarrow{}^4I_{15/2}$ and $^4F_{9/2}\rightarrow{}^4I_{15/2}$ transitions of Er^{3+} ion and the peak positions remain the same. Notably, luminescent intensity for the oleate-free nanoparticles in water increases probably due to absence of the surface oleate. The reason is that organic ligands with high energy C–H or C–C vibrations may lead to fluorescent quench for nearby lanthanide ions.[5]

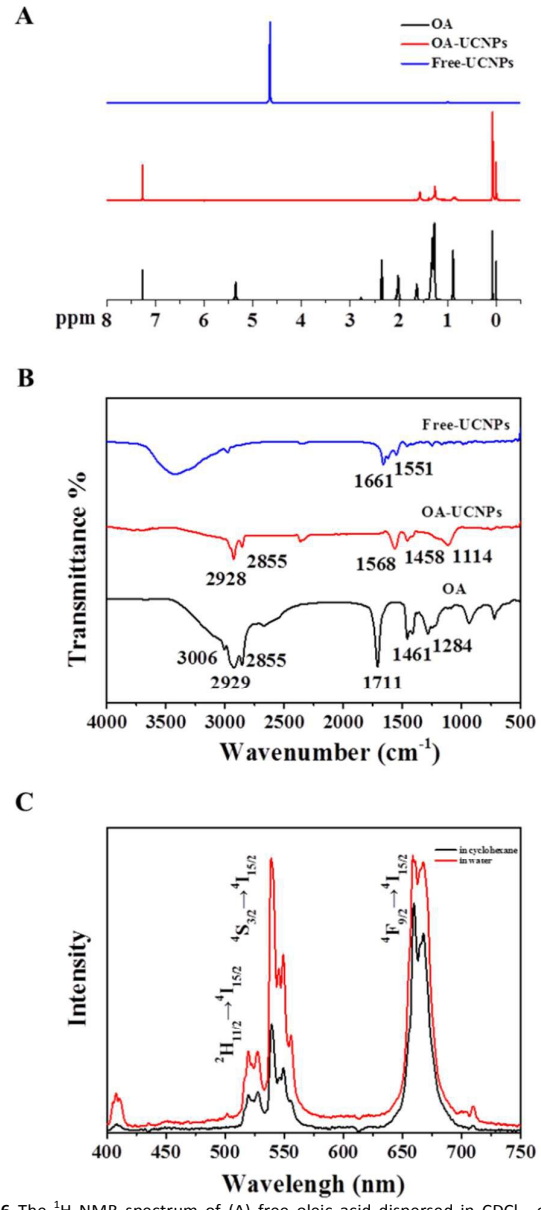

Fig. 6 The ^1H NMR spectrum of (A) free oleic acid dispersed in $CDCl_3$, oleate-capped $NaYF_4$: Er^{3+}, Yb^{3+}@$NaYF_4$ nanospheres dispersed in $CDCl_3$ and $NaYF_4$: Er^{3+}, Yb^{3+} @$NaYF_4$ nanospheres nanoparticles dispersed in D_2O. (B) FTIR spectra of pure oleic acid, oleate-capped $NaYF_4$: Er^{3+}, Yb^{3+}@$NaYF_4$ nanospheres and $NaYF_4$: Er^{3+}, Yb^{3+}@$NaYF_4$ nanospheres nanoparticles. (C) Upconversion spectra of $NaYF_4$: Er^{3+}, Yb^{3+}@$NaYF_4$ nanospheres in water. Nanospheres were excited at 980 nm with a diode laser.

4 Conclusions

Two phases of ytterbium and erbium co-doped sodium yttrium fluoride nanoparticles ($NaYF_4$: Er^{3+}, Yb^{3+}) were synthesized and their luminescence properties, size and morphology under different synthesis conditions were examined. The transformation from the cubic phase to hexagonal phase occurs with the reaction time increasing. β-$NaYF_4$: Er^{3+}, Yb^{3+} have a stronger luminescent intensity than α-$NaYF_4$: Er^{3+}, Yb^{3+}. Upconversion nanoparticles with core-shell structure were prepared to improve their luminescent intensity. The quenching effects can be strongly suppressed by coating a uniform layer of the shell. Finally, water dispersible upconversion nanoparticles with high luminescent intensity were successfully prepared with ligand-free hydrophilic modification.

Acknowledgements

Authors thank the support of National Natural Science Foundation of China (31371014) and Tianjin Natural Science Foundation (13JCYBJC16500).

Notes and references

[a]School of Chemical Engineering and Technology, Tianjin University, Tianjin, 300072, China. E-mail: jinfengxing@tju.edu.cn
[b]College of Material Science and Engineering, Tianjin Polytechnic University, Tianjin, 300387, China.
† These authors equally contributed to this work.

1. J. Zhou, Z. Liu and F. Y. Li, *Chem. Soc. Rev.*, 2012, **41**, 1323-1349.
2. F. Wang, D. Banerjee, Y. S. Liu, X. Y. Chen and X. G. Liu, *Analyst*, 2010, **135**, 1839-1854.
3. T. S. Yang, Q. Liu, J. C. Li, S. Z. Pu, P. Y. Yang and F. Y. Li, *Rsc Adv*, 2014, **4**, 15613-15619.
4. D. R. Larson, W. R. Zipfel, R. M. Williams, S. W. Clark, M. P. Bruchez, F. W. Wise and W. W. Webb, *Science*, 2003, **300**, 1434-1436.
5. Z. Q. Li and Y. Zhang, *Nanotechnology*, 2008, **19**,345606.
6. H. X. Mai, Y. W. Zhang, L. D. Sun and C. H. Yan, *J. Phys. Chem.C.*, 2007, **111**, 13721-13729.
7. H. Y. Xing, W. B. Bu, Q. G. Ren, X. P. Zheng, M. Li, S. J. Zhang, H. Y. Qu, Z. Wang, Y. Q. Hua, K. L. Zhao, L. P. Zhou, W. J. Peng and J. L. Shi, *Biomaterials*, 2012, **33**, 5384-5393.
8. W. Fan, B. Shen, W. Bu, F. Chen, Q. He, K. Zhao, S. Zhang, L. Zhou, W. Peng, Q. Xiao, D. Ni, J. Liu and J. Shi, *Biomaterials*, 2014, **35**, 8992-9002.
9. W. Feng, X. Zhu and F. Li, *Npg Asia Materials*, 2013, **5**,e75.
10. C. Wang, L. Cheng and Z. Liu, *Theranostics*, 2013, **3**, 317-330.
11. L. Cheng, C. Wang and Z. Liu, *Nanoscale*, 2013, **5**, 23-37.
12. J. F. Suyver, J. Grimm, K. W. Kramer and H. U. Gudel, *J.Lumin.*, 2005, **114**, 53-59.
13. H. Dong, L.-D. Sun and C.-H. Yan, *Chem. Soc. Rev.*, 2015, **44**, 1608-1634.
14. J. F. Suyver, J. Grimm, M. K. van Veen, D. Biner, K. W. Kramer and H. U. Gudel, *J.Lumin.*, 2006, **117**, 1-12.

15. J. C. Boyer, L. A. Cuccia and J. A. Capobianco, *Nano. Lett.*, 2007, **7**, 847-852.
16. G. Y. Chen, T. Y. Ohulchanskyy, R. Kumar, H. Agren and P. N. Prasad, *Acs Nano*, 2010, **4**, 3163-3168.
17. P. Qiu, N. Zhou, H. Chen, C. Zhang, G. Gao and D. Cui, *Nanoscale*, 2013, **5**, 11512-11525.
18. M. Haase and H. Schafer, *Angew. Chem. Int. Ed.*, 2011, **50**, 5808-5829.
19. Y. H. Han, S. L. Gai, P. A. Ma, L. Z. Wang, M. L. Zhang, S. H. Huang and P. P. Yang, *Inorg. Chem.*, 2013, **52**, 9184-9191.
20. X. Liang, X. Wang, J. Zhuang, Q. Peng and Y. D. Li, *Adv. Funct.Mater.*, 2007, **17**, 2757-2765.
21. H. X. Mai, Y. W. Zhang, R. Si, Z. G. Yan, L. D. Sun, L. P. You and C. H. Yan, *J. Am. Chem. Soc.*, 2006, **128**, 6426-6436.
22. F. Wang, R. R. Deng, J. Wang, Q. X. Wang, Y. Han, H. M. Zhu, X. Y. Chen and X. G. Liu, *Nat. Mater.*, 2011, **10**, 968-973.
23. F. Wang, J. A. Wang and X. G. Liu, *Angew. Chem. Int. Ed.*, 2010, **49**, 7456-7460.
24. C. Yao, P. Y. Wang, L. Zhou, R. Wang, X. M. Li, D. Y. Zhao and F. Zhang, *Anal. Chem.*, 2014, **86**, 9749-9757.
25. J. C. Boyer, F. Vetrone, L. A. Cuccia and J. A. Capobianco, *J. Am. Chem. Soc.*, 2006, **128**, 7444-7445.
26. Y. W. Zhang, X. Sun, R. Si, L. P. You and C. H. Yan, *J. Am. Chem. Soc.*, 2005, **127**, 3260-3261.
27. X. Li, D. Shen, J. Yang, C. Yao, R. Che, F. Zhang and D. Zhao, *Chem. Mater.*, 2013, **25**, 106-112.
28. R. Abdul Jalil and Y. Zhang, *Biomaterials*, 2008, **29**, 4122-4128.
29. Z. Hou, Y. Zhang, K. Deng, Y. Chen, X. Li, X. Deng, Z. Cheng, H. Lian, C. Li and J. Lin, *ACS nano*, 2015, **9**, 2584-2599.
30. H. S. Qian, H. C. Guo, P. C. Ho, R. Mahendran and Y. Zhang, *Small*, 2009, **5**, 2285-2290.
31. J. Shan, J. Chen, J. Meng, J. Collins, W. Soboyejo, J. S. Friedberg and Y. Ju, *J. Appl. Phys.*, 2008, **104**, 049308.
32. Z. Chen, H. Chen, H. Hu, M. Yu, F. Li, Q. Zhang, Z. Zhou, T. Yi and C. Huang, *J. Am. Chem. Soc.*, 2008, **130**, 3023-3029.
33. L. Xia, X. Kong, X. Liu, L. Tu, Y. Zhang, Y. Chang, K. Liu, D. Shen, H. Zhao and H. Zhang, *Biomaterials*, 2014, **35**, 4146-4156.
34. C. Wang, H. Tao, L. Cheng and Z. Liu, *Biomaterials*, 2011, **32**, 6145-6154.
35. H.-P. Zhou, C.-H. Xu, W. Sun and C.-H. Yan, *Adv. Funct. Mater.*, 2009, **19**, 3892-3900.
36. N. Bogdan, F. Vetrone, G. A. Ozin and J. A. Capobianco, *Nano.Lett.*, 2011, **11**, 835-840.
37. K. W. Kramer, D. Biner, G. Frei, H. U. Gudel, M. P. Hehlen and S. R. Luthi, *Chem. Mater.*, 2004, **16**, 1244-1251.
38. A. Grzechnik, P. Bouvier, W. A. Crichton, L. Farina and J. Kohler, *Solid. State. Sci.*, 2002, **4**, 895-899.
39. Z. Li, Y. Zhang and S. Jiang, *Adv. Mater.*, 2008, **20**, 4765-4769.
40. F. Wang and X. Liu, *Acc. Chem. Res.*, 2014, **47**, 1378-1385.
41. H. Dong, L.-D. Sun and C.-H. Yan, *Nanoscale*, 2013, **5**, 5703-5714.
42. W. B. Niu, S. L. Wu, S. F. Zhang, J. Li and L. A. Li, *Dalton. T*, 2011, **40**, 3305-3314.